Supporting Information for

A Molecular Surface Functionalization Approach to Tuning Nanoparticle Electrocatalysts for Carbon Dioxide Reduction

Zhi Cao,[†] Dohyung Kim,[‡] Dachao Hong,[†] Yi Yu,[†,#] Jun Xu,[†] Song Lin,[†,⊥] Xiaodong Wen,[▽,○] Eva M. Nichols,[†,⊥] Keunhong Jeong,[†] Jeffrey A. Reimer,[†] Peidong Yang,[*,†,‡,#,◆] and Christopher J. Chang,[*,†,§,ǁ,⊥]

[†] Department of Chemistry, [‡] Department of Materials Science and Engineering, [§]Department of Molecular and Cell Biology, and [ǁ]Howard Hughes Medical Institute, University of California, Berkeley, California 94720, United States

[⊥]Chemical Sciences Division and [#]Materials Sciences Division, Lawrence Berkeley National Laboratory, Berkeley, California 94720, United States

[▽] Institute of Coal Chemistry, Chinese Academy of Sciences, Taiyuan, Shanxi 030001, China

[○]Synfuels China, Beijing, 100195, China

[◆] Kavli Energy Nanosciences Institute, Berkeley, California 94720, United States

Table of Contents

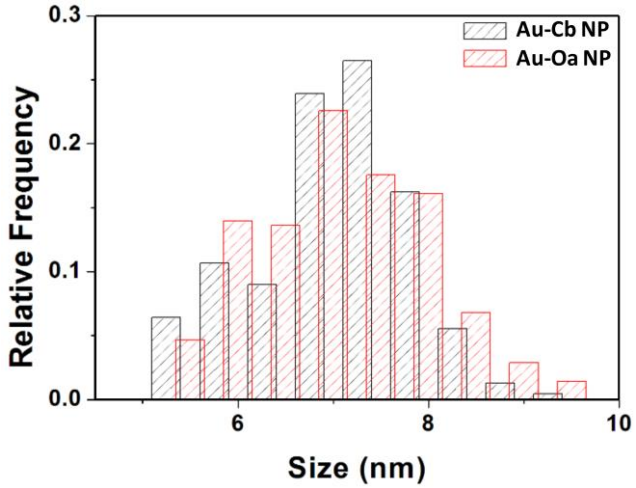

Figure S1. Size distribution of Au-Cb NP (average : 6.9 ± 0.8 nm) and Au-Oa NP (average : 6.9 ± 0.9 nm).

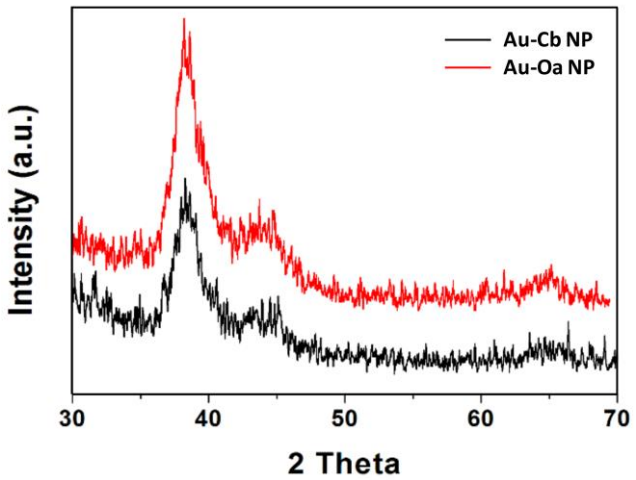

Figure S2. XRD patterns of Au-Cb NP and Au-Oa NP.

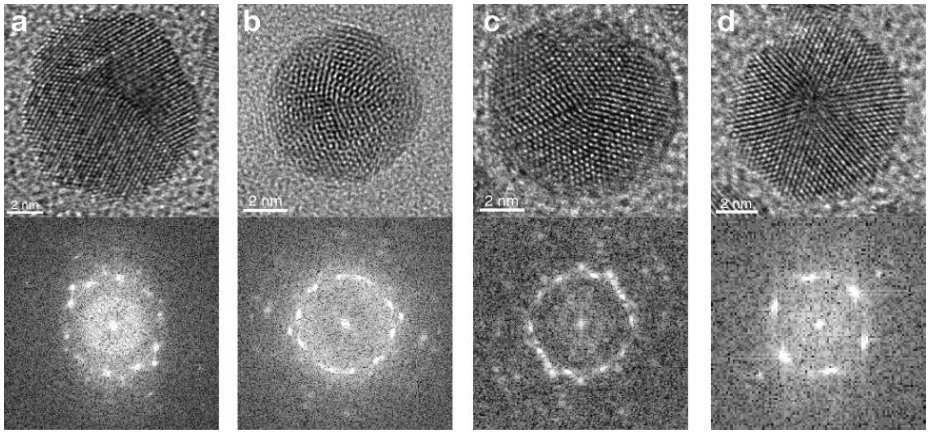

Figure S3. HRTEM image and its FFT of Au-Oa NP with decahedral (a) and icosahedral (b) morphology and Au-Cb NP with decahedral (c) and icosahedral (d) morphology.

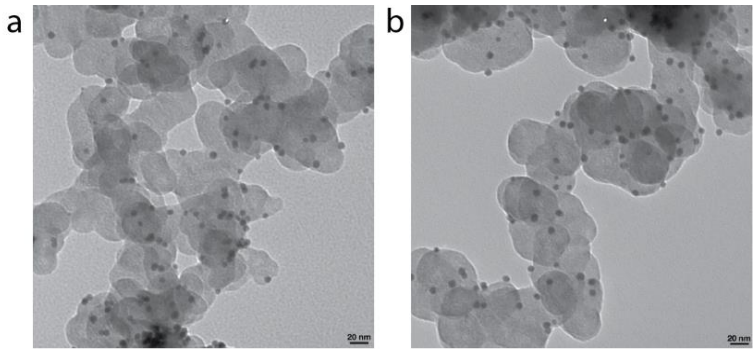

Figure S4. TEM image of (a) Au-Oa NP/C; (b) Au NP/C.

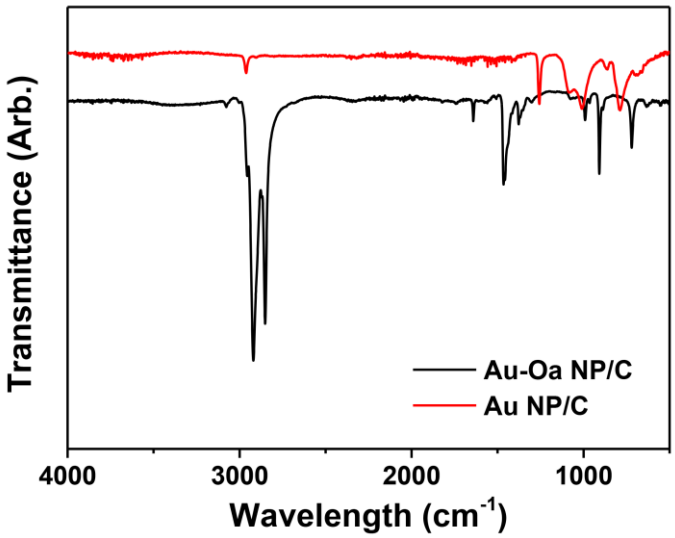

Figure S5. FT-IR spectra of Au-Oa NP/C and Au NP/C.

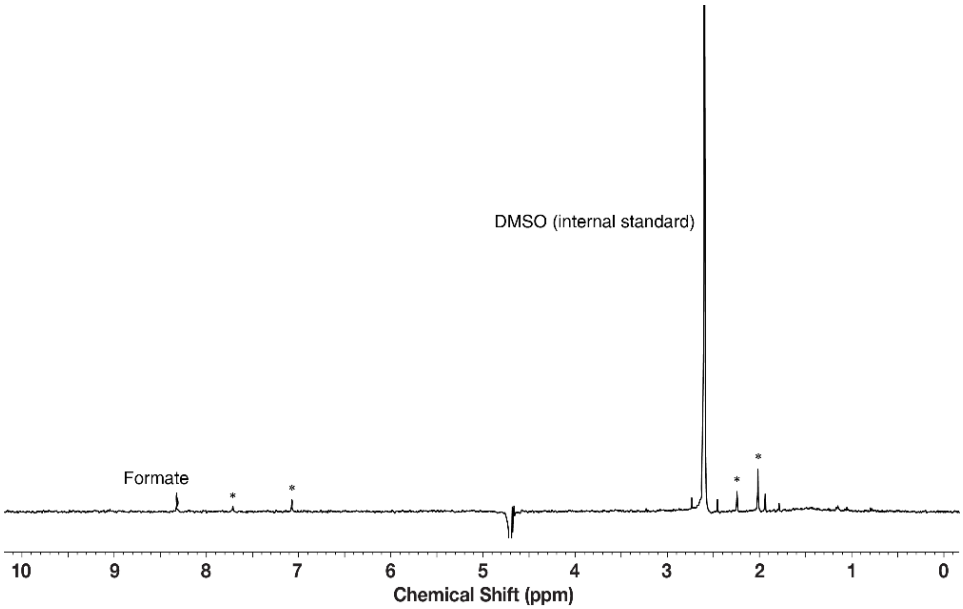

Figure S6. ^{1}H NMR spectra of the electrolyte after electrolysis of Au-Cb NP (at -0.557 V vs RHE) using water-suppression method. The large dip 4.7 ppm is the suppressed water peak. Peaks labeled with asterisks have relative area ratios that match with the number of protons on Cb and are likely to originate from Au-Cb NP that came off from the electrodes due to their tendency to favor polar media.

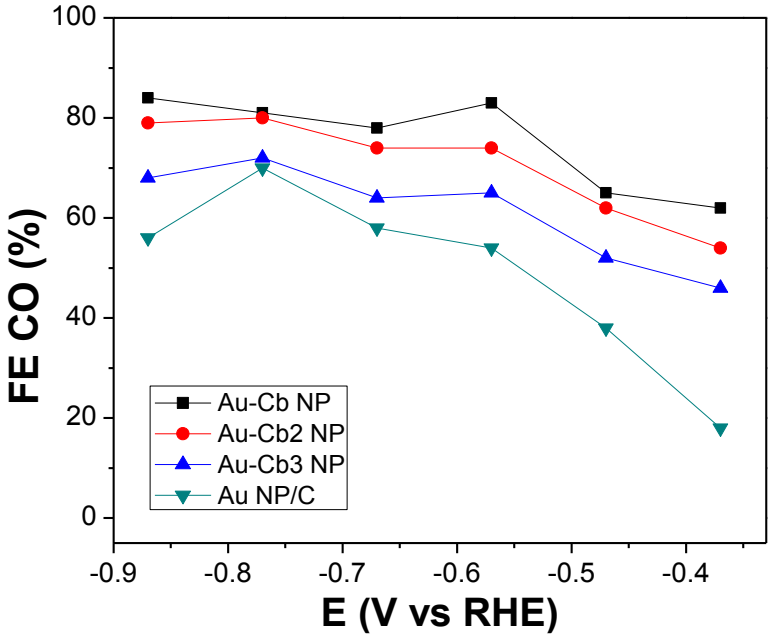

Figure S7. Faradaic efficiencies of produced CO from Au-Cb NP, Au-Cb2 NP, Au-Cb3 NP, and Au NP/C.

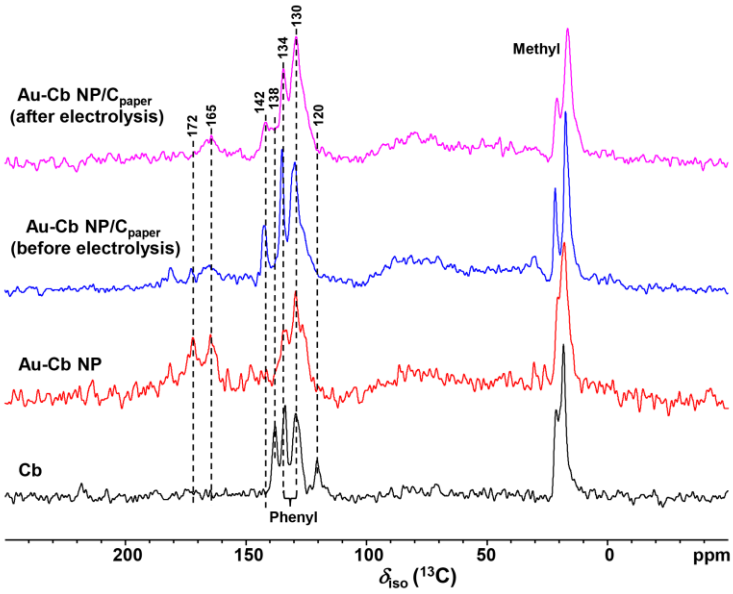

Figure S8. ^{13}C solid-state NMR spectra of free Cb, Au-Cb NP, Au-Cb NP/C_{paper} (before electrolysis), and Au-Cb NP/C_{paper} (after electrolysis). The NMR spectra of Au-Cb NP/C_{paper} before and after electrolysis were measured on the entire working electrode, including both Au-Cb NP and carbon paper. Since carbon paper gives a negligible response as compared with that of Au-Cb NP, the ^{13}C peaks shown in this figure arise from the Au-Cb NP. For the Au-Cb NP/C_{paper} electrode, the diamagnetic contributions of the ring currents in the graphite layers of carbon paper cause the two C peaks at 172 and 165 ppm (arising from the imidazolylidene backbone C) in free Au-Cb NP to shift to 165 and 142 ppm in Au-Cb NP/C_{paper}, respectively. Our observation is similar to the phenomenon that the NMR signals of molecules adsorbed between graphene layers are shifted compared with their freely moving counterparts.[1] However, the ^{13}C NMR feature of Au-Cb NP/C_{paper} after electrolysis is consistent with that of Au-Cb NP/C_{paper} before electrolysis, reflecting the carbene is still bound similarly and stably to the Au surface after electrolysis.

Computational Studies of Cb Binding on Au

To help elucidate the possible origin (geometric effect) of observed improvements in catalytic selectivity and activity of the Au-Cb NPs over their Au NP counterparts, DFT calculations were carried out to track the nanoscale surface-feature change upon carbene functionalization. The Cb molecule binding on gold was examined computationally on a slab model, with the calculated Cb binding mode and associated energies are shown in Fig. S9. The ability of NHC carbenes to act as strong σ-donors and weak π-acceptors results in a very strong carbene-gold bond (bond strength of 150 kJ mol−1).[2] Our computational results, along with others,[3] suggest that the surface gold atom bound to Cb tends to be pulled away from the rest of the metal surface. The calculated distance between this gold atom and the fourth sub-layer gold shell is elongated to 7.935 Å, which is approximately 0.6 Å larger than the unperturbed distance.

All calculations were performed using the plane wave based periodic DFT method as implemented in the Vienna *Ab Initio* Simulation Package (VASP).[4,5] The electron-ion interaction was described with the projector augmented wave (PAW) method.[6,7] The electron exchange and correlation energies were treated within the generalized gradient approximation in the Perdew-Burke-Ernzerhof functional (GGA-PBE).[8] The plane wave basis was set up to 450 eV. Electron smearing was used via the Methfessel-Paxton technique with a smearing width consistent to $\sigma = 0.2$ eV. The average adsorption energy was calculated according to the equation of $\Delta E = [E_{nX/slab} - E_{slab} - E_X]/n$, where $E_{nX/slab}$ is the total energy of the slab with n adsorbed X in its equilibrium geometry, E_{slab} is the total energy of the bare slab, and E_X is the total energy of the free $C_3H_2N_2$-$2C_9H_{11}$ molecule in the gas phase. The calculated lattice constant of cubic Au cell (fcc) is 4.1565 Å, the Au-Au bond is 2.939 Å. The Au (111) is a flat surface, and the unit cell p(6×6) was used in calculations. The 2×2×1 MP k-point sampling was set for the latter. In total, the Au (111) surface has 144 Au atoms, in which 48 Au were fixed.

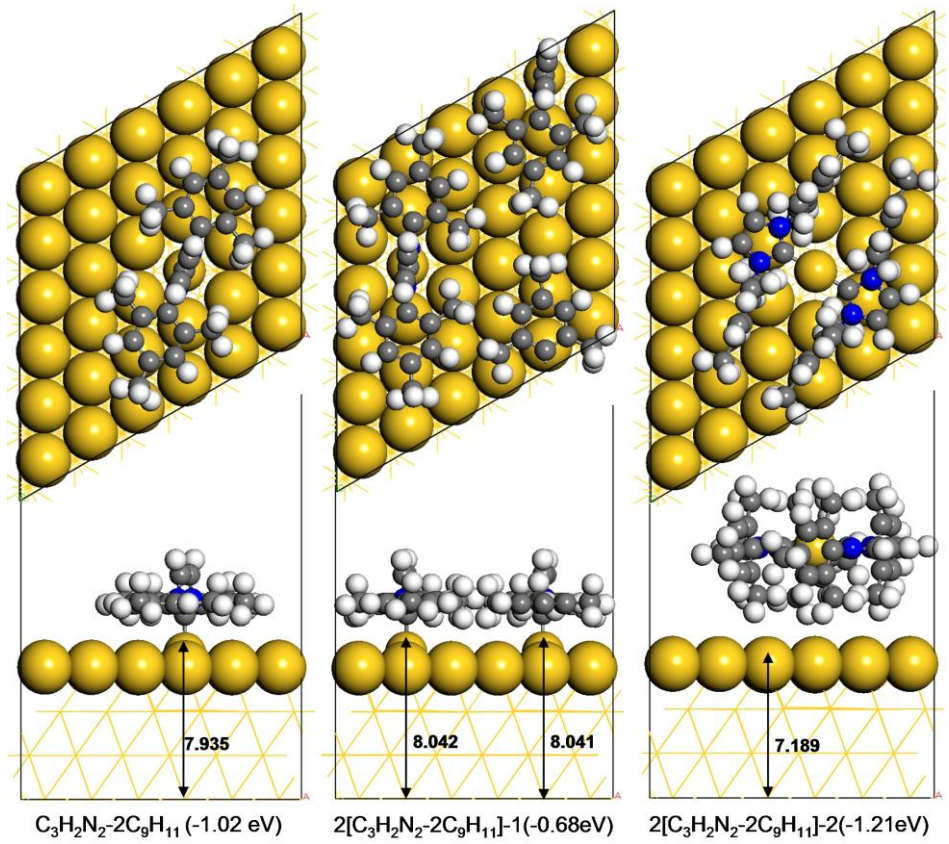

Figure S9. The adsorption structure and energy for $C_3H_4N_2$-$2C_9H_{11}$ (Cb), two $C_3H_4N_2$-$2C_9H_{11}$ (higher density adsorptions of $C_3H_4N_2$-$2C_9H_{11}$ two Cb per unit), and Au-bridged two $C_3H_4N_2$-$2C_9H_{11}$ on Au (111) surface. Clearly, even under more steric repulsion between bound Cbs, the gold atoms can still be pulled out from gold surface. Potentially, an energetically competitive, one gold atom-bridged two molecular $C_3H_4N_2$-$2C_9H_{11}$ equilibrium structure may form by completely pulling out the gold atom from the surface.

References

[1] Deschamps, M.; Gilbert, E.; Azais, P.; Raymundo-Piñero, E.; Ammar, M. R.; Simon, P.; Massiot, D.; Béguin, F. *Nat. Mater.* **2013**, *12*, 351.
[2] Crudden, C. M.; Horton, J. H.; Ebralidze, I. I.; Zenkina, O. V.; McLean, A. B.; Drevniok, B.; She, Z.; Kraatz, H.-B.; Mosey, N. J.; Seki, T. *Nat. Chem.* **2014**, *6*, 409.
[3] Rodríguez-Castillo, M.; Laurencin, D.; Tielens, F.; Van der Lee, A.; Clément, S.; Guari, Y.; Richeter, S. *Dalton Trans.* **2014**, *43*, 5978.
[4] Kresse, G.; Furthmüller, J. *Comput. Mater. Sci.* **1996**, *6*, 15.
[5] Kresse, G.; Furthmüller, J. *Phys. Rev. B* **1996**, *54*, 11169.
[6] Blochl, P.E. *Phys. Rev. B* **1994**, *50*, 17953.
[7] Kresse, G. *Phys. Rev. B* **1999**, *59*, 1758.
[8] Perdew, J.P.; Burke, K.; Ernzerhof, M. *Phys. Rev. Lett.* **1996**, *77*, 3865.